Trees (2026) 40:66
https://doi.org/10.1007/s00468-026-02762-x

ORIGINAL ARTICLE

Thermal tolerance of *Acer campestre* (field maple) under heat and drought stress derived from chlorophyll fluorescence

Ramla Khan[1,2] · **Philip Wheeler**[1] · **David Gowing**[1]

Received: 9 August 2025 / Accepted: 13 March 2026

Abstract

Climate change is increasing the frequency of extreme heat events, making the thermal tolerance of urban trees critical for sustainable city landscapes. We quantified how hydration status influences heat tolerance in Acer campestre (field maple) by measuring chlorophyll-fluorescence based dark-adapted thermal tolerance values for the onset (T_{crit}) and 50% reduction (T_{50}) of photosystem II efficiency. Measurements were taken at four time points under controlled conditions, with the final measurement including drought stress followed by rehydration of the sample leaves. Linear mixed-effects modelling revealed that treatment significantly affected T_{crit} ($F_{(2,49)}=27.6$, $p<0.001$) but not T_{50} ($F_{(2,49)}=2.22$, $p=0.12$). T_{crit} declined from 41.2 to 44.5 °C under well-watered conditions to about 30.4 °C during drought, then recovered to approximately 44.3 °C after 24 h of rehydration. T_{50} remained relatively stable (47–49.9 °C) across treatments. Principal component and clustering analyses confirmed hydration status as the main driver of variation (PC1 = 80.4% of variance; PERMANOVA $F=5.47$, $p=0.001$). A positive correlation between T_{crit} and T_{50} ($r=0.61$, $p<0.01$) indicated coordinated but distinct protective mechanisms operating across stress levels. These findings demonstrate that short-term hydration has a greater influence on photosynthetic heat tolerance than prior drought exposure. *Acer campestre* shows high physiological plasticity, with rapid recovery of T_{crit} after rehydration, suggesting that maintaining soil moisture through targeted irrigation could significantly enhance tree resilience to increasing urban heat extremes.

Keywords Acer campestre · Thermal tolerance · Chlorophyll fluorescence · Photosystem II · Urban forestry · Climate change

Introduction

Urban environments increasingly experience excessive temperatures due to climate change and the urban heat island effect, placing urban vegetation under unprecedented thermal stress.

(IPCC, 2021, 2023; Kendon et al. 2022). As extreme heat events become more frequent and intense, the physiological limits of urban trees are tested, threatening their survival and capacity to provide ecosystem services (Coutts et al. 2016; Grilo et al. 2025). While urban trees can significantly mitigate local temperatures through shading and evapotranspiration (Meier and Scherer 2012), their ability depends critically on maintaining their physiological function during heat stress.

Chlorophyll fluorescence offers a sensitive, non-invasive approach for quantifying plant responses to thermal stress by measuring photosystem II efficiency, which typically experiences damage before other physiological systems (Murchie and Lawson 2013). This approach yields two particularly valuable thermal tolerance metrics: critical temperature (T_{crit}), indicating the onset of photosynthetic decline (Kullberg and Feeley 2024; Perez & Feeley, 2020), and T_{50}, the temperature at which photosynthetic function is reduced by half (Perez and Feeley 2020b).

Previous research has documented considerable variation in thermal tolerance among tree species, with T_{50} generally between 45 and 54 °C and T_{crit} between 41 and 51 °C (Leon-Garcia and Lasso 2019; O'sullivan et al. 2017). These studies have identified interspecific differences in thermal tolerance, often linked to species' native growing conditions

✉ Ramla Khan
ramla.khan@ndorms.ox.ac.uk

[1] School of Earth, Environment and Ecosystem Sciences, The Open University, Milton Keynes, UK

[2] Health Data Sciences, University of Oxford, Oxford, UK

Published online: 17 April 2026

and physiological adaptations. Studies suggest that thermal tolerance is not fixed but dynamic, responding to both genetic factors and environmental conditions. For instance, studies in agricultural and forest systems have documented significant variation in thermal tolerance within species (Posch et al. 2022) and in response to environmental gradients such as elevation (Feeley et al. 2020). Researchers have also begun to explore potential relationships between drought tolerance and heat tolerance, suggesting complex interactions between water status and thermal resilience (Kunert et al. 2022).

Many existing studies assess thermal tolerance under standardised, optimal conditions, often using well-watered plants and fixed environments that do not fully capture the dynamic and co-occurring stressors typical of urban settings. This can lead to an overestimation of thermal resilience, particularly where drought and heat stress interact. Drought has long been recognised to intensify the effects of heat stress by limiting CO_2 diffusion, reducing stomatal conductance, and destabilising the repair of photosystem II (Flexas 2002). These interactions can substantially amplify photochemical damage under high temperatures. In this study, we test the hypothesis that the thermal tolerance of *Acer campestre* is governed primarily by its immediate hydration status rather than by prior drought exposure. We propose that water availability at the time of heat stress is the key factor regulating photosystem II stability and recovery and therefore represents the dominant control on short-term thermal resilience.

Although increasingly recognised, the role of hydration status in modulating plant thermal tolerance remains underexplored. Unlike controlled experimental conditions, urban trees frequently experience varying degrees of water stress that may significantly alter their effective thermal thresholds. Recent investigations suggest that immediate hydration status may be a primary determinant of thermal tolerance, potentially even surpassing species-specific adaptations or drought acclimation in importance (Münchinger et al. 2023). This hypothesis remains inadequately tested, particularly for common urban tree species under field-relevant conditions.

This knowledge gap has significant implications for urban forestry practice. Current approaches to species selection and management often rely on thermal tolerance values derived under optimal conditions, potentially misrepresenting performance during real-world heat events where water stress frequently co-occurs. Understanding how hydration status modulates thermal thresholds would enable more accurate vulnerability assessments and targeted irrigation interventions during extreme heat.

We quantified the relationship between hydration status and thermal tolerance in *Acer campestre* (field maple), a widely planted urban tree in the UK and Europe. Through controlled experimental manipulations of both water availability and temperature exposure, we examine how chlorophyll fluorescence parameters respond to heat stress under varying hydration conditions. Unlike previous studies that typically assess thermal tolerance at a single point in time or hydration state, our experimental design specifically isolates the effects of immediate hydration status versus prior drought conditioning, allowing us to disaggregate their relative contributions to thermal resilience.

Using multivariate statistical techniques, including generalised mixed models, principal component analysis and clustering, we identify the primary drivers of variation in thermal response patterns. This approach reveals whether thermal tolerance in Acer campestre is primarily determined by fixed, species-level characteristics or is dynamically regulated by hydration status, a distinction with important implications for urban tree management under climate change.

Specifically, our research aims to quantify variation in T_{crit} and T_{50} across hydration states; evaluate the relative effects of hydration and prior drought; and assess implications for urban tree management under extreme heat.

Methods

Thermal tolerance was assessed at four time points on eight field maple trees growing in containers/pots (Fig. 1a) on the Open University grounds in Milton Keynes, UK, using the OS5p+ chlorophyll modulated fluorometer (ADC, Hoddesdon, UK) (Opti-Sciences 2013).

Tree species of study

Citizen science based project, Treezilla, suggests *Acer campestre* is a common urban tree species in the United Kingdom (Treezilla 2024). It is a deciduous tree native to the British Isles and widespread across Europe. Typically reaching 12–15 m in height (up to 25 m in some cases), it is common in hedgerows, woodland edges, and parklands. The species has light grey, flaking bark and a rounded, low-branching crown. Its foliage emerges bright green in spring, turning golden to red in autumn. Small yellow-green flowers appear in late April, followed by twin-winged samaras that disperse by wind in October (Zecchin et al. 2016).

Controlled mesocosm system

The trees were grown in 90-L pots arranged in a 2 × 4 grid and connected to an automated mesocosm irrigation system modified from Araya et al. (2010) shown in Fig. 1a. The

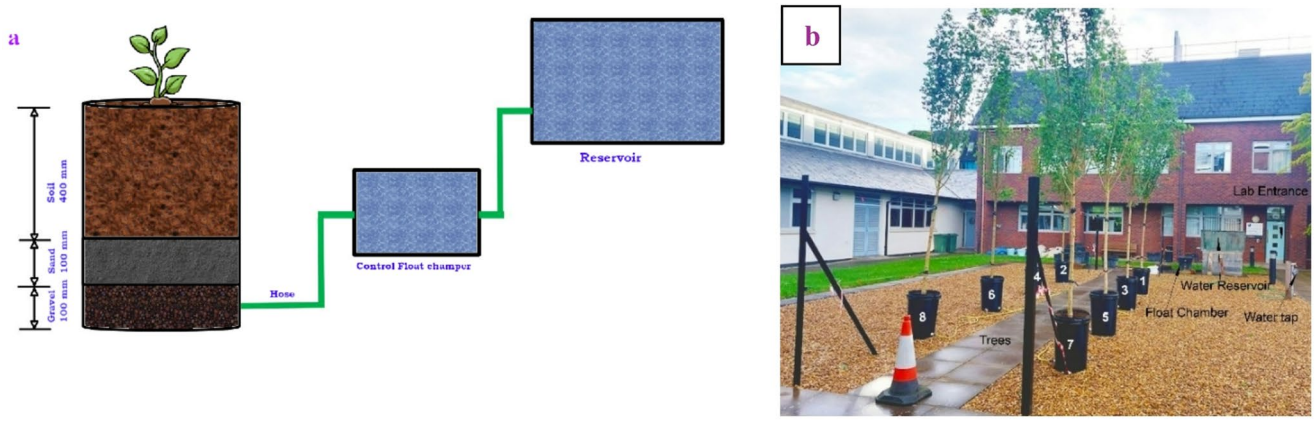

Fig. 1 Outdoor experimental setup, **a**) Controlled water depth system, **b**) Numbered field maple trees with labelled water reservoir and float chambers near the marked lab entrance

system maintained consistent soil moisture and minimised water stress during thermal tolerance experiments. Each pot contained stratified substrate layers comprising coarse gravel (10 cm), fine sand (10 cm), and potting soil mixed with field soil (55 cm), separated by a permeable weed membrane to allow drainage and water movement (Fig. 1b). The water table was maintained at approximately 50 cm below the soil surface via 12 mm hoses linked to a central reservoir with float valves. Water levels were visually checked daily in the central reservoir and refilled twice weekly. The pots were positioned in full sun with 1.5 m spacing to prevent shading, and trees were stabilised using horizontal galvanised steel cables to reduce wind disturbance. A weather station located 2 m above canopy height continuously recorded temperature, precipitation, humidity, solar radiation, and wind speed, ensuring controlled yet field-relevant growing conditions.

The first three measurements (T1, T2, T3) were conducted under ambient summer conditions in July 2023 (mean air temperature = 17.6 °C, range 8.7–29.6 °C; mean relative humidity = 76%), and the last measurement (T4) took place in late August 2023 (mean air temperature = 16.5 °C, range 9.1–27.8 °C; mean relative humidity = 79%), with no rainfall recorded during the last experimental period. The details of the weather conditions, as recorded by the weather station, are provided as supplementary data with this work.

The first three measurements were each separated by approximately ten days. Before the final measurement, drought stress was imposed by withholding irrigation for five consecutive days while the trees remained outdoors. No rainfall occurred during this period, and visible leaf wilting was observed in some trees, consistent with the possible development of some degree of water deficit. Given that the trees were grown in 90-litre pots with a finite soil volume, five consecutive days without irrigation was considered likely to produce meaningful soil moisture depletion, though the severity of any water deficit cannot be formally quantified in the absence of direct soil or leaf water potential measurements. Although soil water content and leaf water potential were not directly measured, drought intensity was inferred from both visual symptoms and Fv/Fm decline.

Controlled experiments for thermal tolerance

Branches approximately 20–25 cm in length and 0.5–0.8 cm in diameter were collected from the trees and brought to the laboratory for fluorescence analysis. The tips of the stem were cut under water to trap the transpiration bubble. Leaf discs (2 cm in diameter; one disc per temperature treatment per tree) from these branches were extracted using a cork borer to ensure uniform sampling. To maintain aerobic conditions and prevent anaerobiosis during heating, the leaf discs were enclosed within a tea cloth, with one layer placed on the adaxial side and another on the abaxial side. The wrapped discs were then placed in a sealed plastic bag and fully submerged in a water bath, secured with weights to ensure complete immersion while preventing moisture contamination.

The maximum quantum yield of photosystem II (F_v/F_m) was initially measured at 20 °C to establish baseline values and verify the physiological integrity of the sampled leaves. Variation in baseline Fv/Fm values at 20 °C reflects natural heterogeneity among sampled leaves (e.g. differences in leaf age and pre-sampling hydration status), whereas subsequent dark adaptation and rehydration under controlled laboratory conditions standardise physiological state before recovery measurements. The leaf discs were then subjected to controlled heat treatments in a darkened water bath for fifteen minutes. Treatment temperatures ranged from 37 °C to 60 °C in 4 °C increments.

Following heat treatments, the leaf discs were retrieved using protective gloves to prevent physical damage and

transferred onto petri dishes lined with moistened paper towels soaked in distilled water. The samples were subsequently acclimated in a light-free environment under a dark cloth for fifteen minutes before measuring F_v/F_m using an OS5p+ fluorometer (Opti-Sciences 2013). After the initial fluorescence measurements, the leaf discs were stored in petri dishes with closed lids under laboratory conditions (Fig. 2) to undergo a 24-hour recovery phase. Post-recovery F_v/F_m measurements were recorded to evaluate the extent of recovery or degradation in photosynthetic efficiency.

Estimating the dark-adapted thermotolerance

To estimate T_{crit} and T_{50}, a logistic nonlinear least squares model was used to characterise the relationship between F_v/F_m and treatment temperature for each sample (Kunert et al. 2022; Münchinger et al. 2023; Tiwari et al. 2021). Because T_{crit} and T_{50} were derived from the fitted temperature–response curves rather than from absolute Fv/Fm values at 20 °C, variation in baseline fluorescence among treatments does not bias the dark-adapted thermotolerance estimation. The modelling was implemented using the 'nls' function within the R 'stats' package (R Core Team, 2025). T_{crit} was defined as the temperature at which a noticeable decline in Fv/Fm began, identified by detecting the point where the slope of the Fv/Fm–temperature curve reached 15% of its steepest (most negative) value (Kullberg and Feeley 2024; Perez & Feeley, 2020). T_{50} was calculated using Eq. 1 as the temperature at which Fv/Fm dropped to 50% of the average value observed in the control (non-stressed) treatment (Perez & Feeley, 2020).

Fig. 2 Samples left overnight in the lab, with the numbers representing the eight trees and the value of the temperature treatment at the top. A proper cautionary sign was left to avoid accidental merging of the samples

$$\frac{F_v}{F_m} = c + \frac{d-c}{1 + Exp[b\log\left(\frac{T}{T_{50}}\right)]} \quad (1)$$

In Eq. 1, T denotes temperature, while *c* represents the F_v/F_m value at the lower plateau, and d corresponds to the higher plateau. T_{50} refers to the temperature at which F_v/F_m declines to 50% of the total reduction, and b signifies the slope of the curve at $T = T_{50}$.

The dark-adapted thermal tolerance (T_{crit} and T_{50}) were extracted from fitted temperature–response curves and are therefore robust to variation in absolute Fv/Fm values at 20 °C. Because measurements were repeated on the same individual trees across time points, non-independence of observations was addressed in subsequent analyses using linear mixed-effects models.

Linear mixed-effects modelling

Since the same individual trees were measured across multiple treatments, we used linear mixed-effects models (LMMs) to account for the non-independence of repeated measures. Models were fitted separately for T_{crit} and T_{50} using the lmer() function from the R package 'lme4' (Bates et al. 2015), with treatment (Initial, After 24 h, and Initial Drought) as a fixed effect and Tree ID as a random intercept. Type III ANOVA tests from the package 'lmerTest' (Kuznetsova et al. 2017) provided significance for fixed effects, and post-hoc pairwise comparisons were conducted using 'emmeans' with Tukey adjustment for multiple testing (Lenth 2017). Residuals were visually inspected to verify normality and homoscedasticity.

Principal component and cluster analysis

To explore multivariate patterns in physiological responses across treatments and time points, a Principal Component Analysis (PCA) was conducted on scaled data using the 'prcomp()' function in R from the base package 'stats' (R Core Team, 2025). This dimensionality reduction technique was used to identify the primary axes of variation.

Unsupervised k-means clustering was applied to identify natural groupings in the data using the 'stats' package. The optimal number of clusters (K) was determined using the silhouette method from the 'cluster' package (Mächler et al. 2012). To statistically test treatment and cluster differences in multivariate space, Permutational Multivariate Analysis of Variance (PERMANOVA) was conducted using the 'adonis2()' function in the 'Vegan' package (Oksanen et al. 2025). The distance matrix was calculated using Euclidean distances on scaled variables.

Results

The dark-adapted thermal tolerance values

In our study, mean critical temperature (T_{crit}) and half-inactivation temperature (T_{50}) values varied across trials and hydration treatments, reflecting dynamic changes in thermal tolerance (Table 1; Fig. 3). Across all time points, T_{crit} ranged from 30.4 °C under drought to 44.5 °C after rehydration, while T_{50} remained comparatively stable between 47.0 and 49.9 °C. The 24-h rehydration consistently increased both dark-adapted thermal tolerance values, with the largest recovery observed under drought (T4), where T_{crit} rose from 30.4 °C to 44.3 °C and T_{50} increased from 47.0 °C to 49.2 °C. These results confirm that short-term hydration rapidly restores thermal tolerance.

Linear mixed-effects analysis of treatment effects

To account for repeated measurements on the same trees, linear mixed-effects models (LMMs) were used with treatment as a fixed effect and Tree ID as a random intercept. The LMM revealed a statistically significant effect of treatment on T_{crit} ($F_{2,49} = 27.6$, $p < 0.001$) but not on T_{50} ($F_{2,49} = 2.22$, $p = 0.12$). Tukey-adjusted pairwise comparisons showed that T_{crit} increased by + 3.44 °C ($p = 0.031$) after 24 h rehydration and decreased by − 10.42 °C ($p < 0.001$) under drought relative to initial conditions. No significant pairwise differences were observed for T_{50}.

The random intercept explained only 8% of the variance in T_{crit} and 3% in T_{50}, indicating consistent treatment effects across the trees.

Correlation between T_{crit} and T_{50}

A Pearson correlation analysis revealed a significant positive association between T_{crit} and T_{50} ($r = 0.61$, $t = 6.03$, $df = 62$, $p < 0.01$; 95% CI: 0.43–0.74 °C; Fig. 4). This positive association indicates that T_{crit} and T_{50} tend to shift in the same direction across treatments, reflecting coordinated responses to thermal stress. However, the differing magnitudes and treatment sensitivities of the two metrics indicate that they capture distinct physiological processes rather than a single continuum of thermal tolerance. The distinct response magnitudes underscore that these metrics capture complementary aspects of thermal stress physiology.

Principal component and cluster analysis

To explore underlying patterns in dark-adapted thermal tolerance, a Principal Component Analysis (PCA) was performed on T_{crit} and T_{50} values. K-means clustering, validated by silhouette analysis (optimal $K = 2$, score = 0.46), separated samples into two distinct physiological groups (Fig. 5). The first principal component (PC1) explained 82.5% of the total variance, primarily capturing differences in T_{crit}, while PC2 accounted for 17.5% (Fig. 6).

Cluster 1 consisted predominantly of post-hydration samples and exhibited consistently high thermal tolerance (mean T_{crit}: 44.1 °C, T_{50}: 49.2 °C). Cluster 2 included mainly pre-hydration measurements and was characterised by lower values (T_{crit}: 33.2 °C, T_{50}: 46.2 °C; Fig. 6). The clear separation between these clusters reflects the dominant role of water availability in driving physiological plasticity in dark-adapted thermal tolerance values.

Multivariate differences between treatments

To statistically evaluate the combined influence of hydration and experimental treatment, a PERMANOVA was conducted on scaled T_{crit} and T_{50} values using Euclidean distances. The analysis confirmed significant treatment effects ($F = 5.46$, $R^2 = 0.39$, $p = 0.001$), indicating that variation in thermal responses was strongly explained by hydration status and trial conditions.

Table 1 T_{crit} and T_{50} measurements across four time points, with measurements taken initially and after a 24-hour hydration period

Trial date	Treatment	T_{crit} mean (°C)	T_{crit} 95% CI lower	T_{crit} 95% CI upper	T_{50} mean (°C)	T_{50} 95% CI lower	T_{50} 95% CI upper
03 Jul 2023	Initial	41.2	32.3	49.9	49.9	46.9	52.5
	After 24 h rehydration	43.4	40.8	47.3	48.5	46.4	49.7
13 Jul 2023	Initial	40.2	34.1	47.3	47.9	46.5	50
	After 24 h rehydration	44.5	40.8	47.7	48.2	45.6	51.1
23 Jul 2023	Initial	41.2	30.8	48.5	48	43.7	50
	After 24 h rehydration	44.1	39.5	47.8	48.4	46.8	49.6
28 Aug 2023	Initial (drought)	30.4	21.2	39.5	47	42.9	51.2
	After 24 h rehydration	44.3	38.4	48.3	49.2	47.9	51.3

Values are shown with 95% confidence intervals

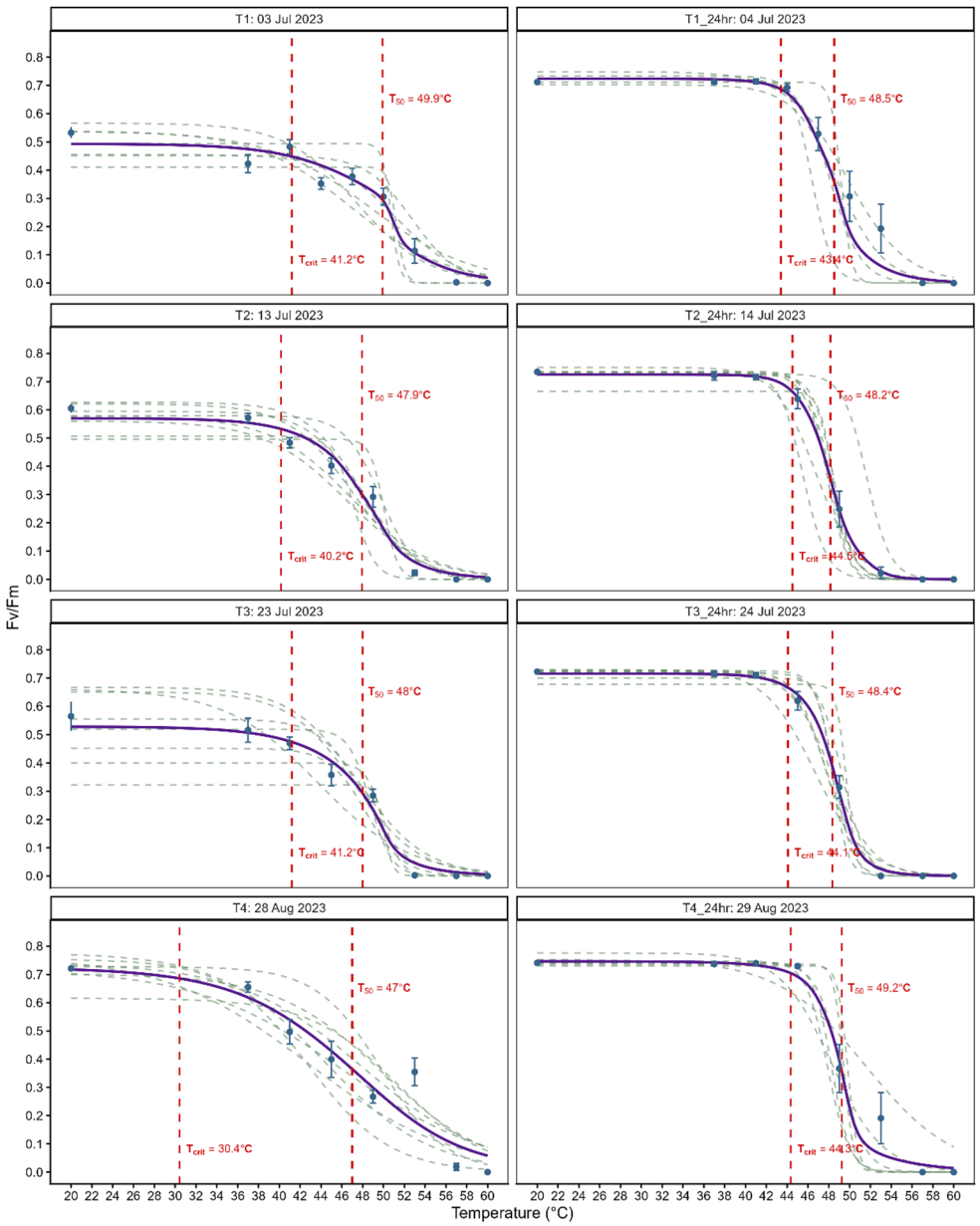

Fig. 3 Temperature response curves of maximum quantum yield (Fv/Fm) for Acer campestre across four time points. The solid purple line represents the mean response curve across all replicates, while the green dotted lines show individual tree replicates ($n=8$). Vertical red dashed lines indicate the temperature thresholds, T_{crit} and T_{50}

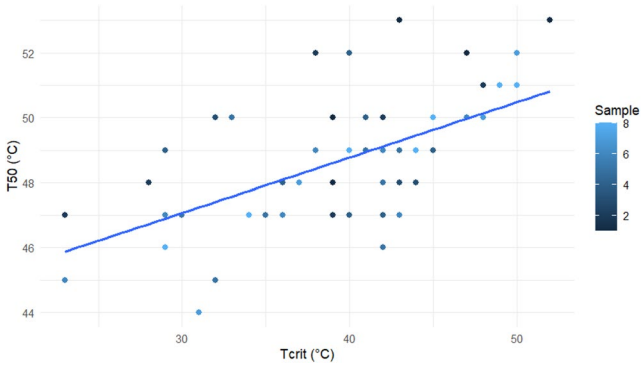

Fig. 4 Pearson correlation between T_{50} and T_{crit} values. The samples in the legend represent the eight replicates across each temperature treatment

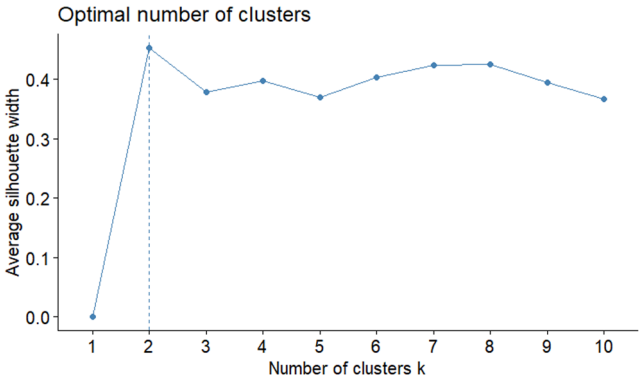

Fig. 5 Number of clusters derived through the silhouette method

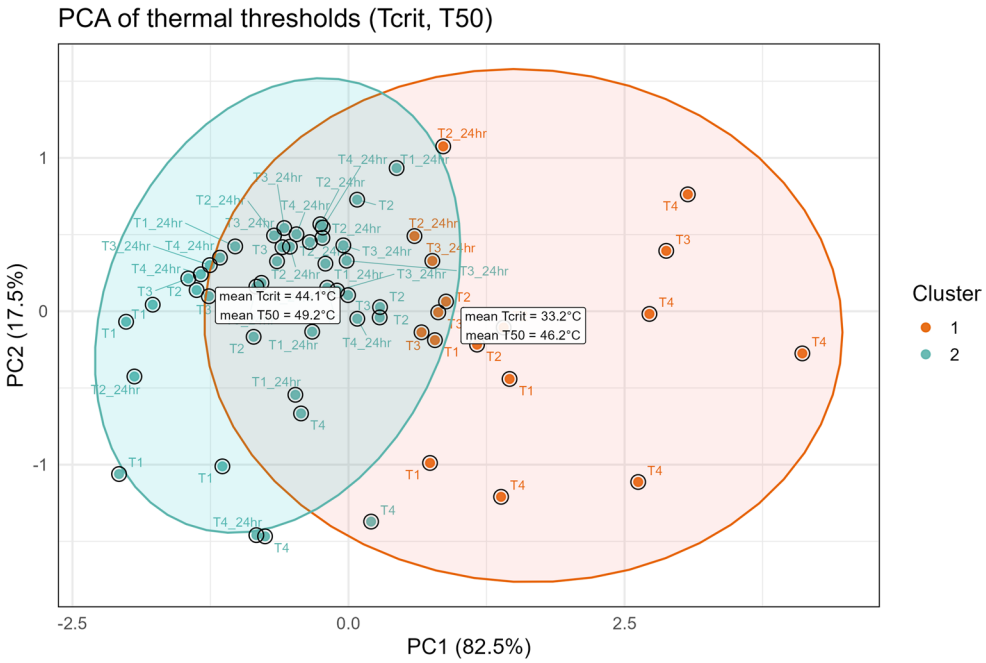

Fig. 6 Principal Component Analysis (PCA) plot showing sample distribution along PC1 (82.5%) and PC2 (17.5%). Cluster 1 is colour-coded in red and Cluster 2 in blue, with the Ellipses representing the 95% confidence intervals for each cluster. Labels "T1", "T2", "T3", and "T4" present the measurements at different time points, and their corresponding 24-hour post-hydration measurements. All points represent replicate-level threshold estimates; no binning or discretisation of T_{crit} or T_{50} values was applied

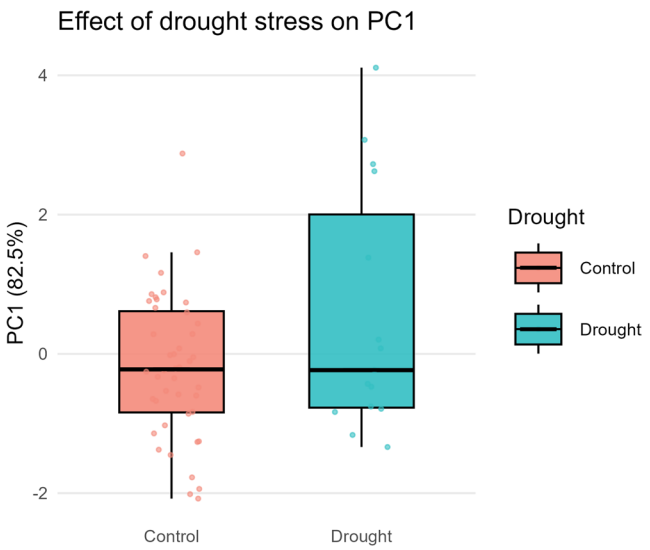

Fig. 7 Boxplot illustrating the effect of drought stress on PC1 (82.5%) in blue, while the other measurements (control) are in red

Impact of drought treatments

Drought-stressed samples (T4) showed greater dispersion in the dark-adapted thermal tolerance values than controls (Fig. 7). However, PCA revealed substantial overlap between drought and control treatments along PC1, indicating that hydration status had a more immediate and pronounced effect on thermal threshold values than drought stress alone.

Discussion

This study investigated the thermal tolerance of *Acer campestre* under heat and drought stress through a series of controlled laboratory experiments at different time points, incorporating chlorophyll fluorescence-derived metrics (T_{crit} and T_{50}). The results demonstrate pronounced physiological plasticity in T_{crit} driven by short-term changes in water availability, whereas T_{50} remained comparatively stable. This pattern highlights the dominant role of immediate hydration in determining photosystem II (PSII) resilience and clarifies the different physiological meanings of these two metrics.

Across all experimental trials, T_{crit} responded strongly to water status, falling to 30.4 °C during drought and rising above 44 °C after rehydration. Linear mixed-effects models confirmed that treatment had a highly significant effect on T_{crit} ($F_{(2,49)}=27.6$, $p<0.001$) but not on T_{50} ($F_{(2,49)}=2.22$, $p=0.12$). Post-hoc contrasts showed that rehydrated trees had significantly higher T_{crit} than initial or drought-stressed trees (+3.4 °C and +13.9 °C, respectively). These results align with mechanistic evidence that hydration maintains cellular turgor and membrane stability, supporting PSII enzyme function and repair (Kim and Portis 2005). The rapid recovery observed here likely reflects the re-establishment of these processes rather than de novo protein synthesis, which would require longer timescales. The weaker response of T_{50} indicates that protection against catastrophic PSII failure relies more on constitutive structural and biochemical defences that are less affected by short-term water status. Although mean T50 values appeared marginally

higher under drought, this difference was not statistically significant and likely reflects variability among replicate curve fits rather than enhanced thermal tolerance. Similar decoupling between early photochemical decline and irreversible damage has been reported in other woody species (Sharkey 2005). Thus, T_{crit} acts as a sensitive indicator of current physiological condition, whereas T_{50} better represents intrinsic thermal limits. Recognising this distinction helps explain inconsistencies among species-level comparisons when hydration status is not explicitly controlled.

It should be noted that the T_{crit} reported here is derived from dark-adapted Fv/Fm and is distinct from the classical F0-rise-based T_{crit} (Schreiber & Berry, 1977), which identifies the onset of irreversible PSII membrane damage during continuous heating. The Fv/Fm-based approach used here, following Perez & Feeley (2020) and Kullberg et al. (2024), captures the earliest detectable departure from baseline photosynthetic function and represents an increasingly adopted standard in comparative thermal tolerance studies. Hydrated *Acer campestre* maintained T_{crit} values of 42–44 °C, comparable to moderately heat-tolerant deciduous species (Slot et al. 2021), but drought reduced this threshold by more than 10 °C, placing water-limited individuals in a vulnerability range where urban surface temperatures commonly exceed 40 °C. T_{50} values (47–50 °C) position the species mid-range among temperate trees (Gillner et al. 2015; Teskey et al. 2015). These data indicate that *Acer campestre* can withstand brief heat events when adequately hydrated but is susceptible to prolonged heat combined with moisture deficit.

The wide variability of Fv/Fm values observed at 20 °C in our results reflect natural leaf-level heterogeneity before treatment, whereas the convergence of values after recovery results from standardised dark adaptation and rehydration under controlled laboratory conditions. Hydration-driven variation in T_{crit} reflects fast physiological adjustments, membrane stabilisation, osmotic balance, and restoration of electron transport efficiency, that precede slower acclimatory responses such as heat-shock protein induction. The substantial recovery after rehydration suggests a strong capacity for short-term resilience, while the incomplete recovery after drought implies limits to this plasticity under repeated or extended stress. These findings underscore that water availability, rather than prior drought history, governs immediate thermal resilience. However, because all trees were subjected to the same drought treatment, these patterns should be interpreted as treatment-driven rather than reflecting intrinsic differences among individual trees; disentangling individual drought legacy effects would require a split-drought experimental design, which was beyond the scope of the present study.

The strong dependence of T_{crit} on hydration emphasises that irrigation management is as critical as species selection for sustaining urban forest function. Ensuring adequate soil moisture during heat waves can prevent PSII impairment and accelerate post-stress recovery. However, this controlled, potted-tree experiment cannot fully replicate complex urban rooting environments and microclimates. Future field studies across soil-moisture gradients and repeated stress cycles will be needed to assess cumulative and seasonal acclimation effects. Investigating underlying cellular mechanisms could also clarify why T_{crit} is more labile than T_{50}.

Conclusion

Acer campestre shows marked short-term physiological plasticity in thermal tolerance controlled by hydration status. Linear mixed-effects modelling revealed that rehydration significantly increased T_{crit}, whereas drought caused a substantial decline, confirming water availability as the dominant factor influencing PSII stability. In contrast, T_{50} remained largely constant across treatments, suggesting that mechanisms protecting against catastrophic heat damage are less responsive to immediate hydration. Hence, it can be stated.

hydration regulates the threshold for initial stress onset but not the ultimate limit of photosynthetic failure. Under drought, T_{crit} can drop to levels that overlap with common urban canopy temperatures, highlighting the potential vulnerability of un-watered street trees. Rapid recovery following rehydration indicates that timely irrigation could markedly enhance resilience during extreme heat.

As urban heat and drought intensify, integrating hydration-dependent physiological data into species selection and irrigation scheduling will be essential for maintaining healthy urban forests. Future research should extend this approach across additional species and repeated stress cycles to identify traits conferring sustained thermal tolerance under fluctuating water availability.

Author contributions Ramla Khan wrote the draft, collected the data, and performed analysis as part of her PhD work. David Gowing and Philip Wheeler, in the position of supervisors, revised the document, gave suggestions for the analysis protocol and data collection.

Funding The research was funded by the Engineering and Physical Sciences Research Council of the UK.

Data availability The data and code that support the findings of this study are openly available at Zenodo on the link: 10.5281/zenodo.15376888.

Declarations

Competing interests The authors have no relevant financial or non-financial interests to disclose.

Consent to Publish Not applicable.

Ethics and consent to Participate The plant material used in this study, *Acer campestre*, was cultivated on the Open University grounds and not collected from the wild. All procedures complied with local and national guidelines for plant research. No permits or licenses were required.

References

Araya YN, Gowing DJ, Dise N (2010) A controlled water-table depth system to study the influence of fine-scale differences in water regime for plant growth. Aquat Bot 92(1):70–74. https://doi.org/10.1016/j.aquabot.2009.10.004

Bates D, Mächler M, Bolker B, Walker S (2015) Fitting Linear Mixed-Effects Models Using lme4. J Stat Softw 67(1). https://doi.org/10.18637/jss.v067.i01

Coutts AM, White EC, Tapper NJ, Beringer J, Livesley SJ (2016) Temperature and human thermal comfort effects of street trees across three contrasting street canyon environments. Theoret Appl Climatol 124(1–2):55–68. https://doi.org/10.1007/s00704-015-1409-y

Feeley K, Martinez-Villa J, Perez T, Silva Duque A, Triviño Gonzalez D, Duque A (2020) The Thermal Tolerances, Distributions, and Performances of Tropical Montane Tree Species. Front Forests Global Change 3. https://doi.org/10.3389/ffgc.2020.00025

Flexas J (2002) Drought-inhibition of Photosynthesis in C3 Plants: Stomatal and Non-stomatal Limitations Revisited. Ann Botany 89(2):183–189. https://doi.org/10.1093/aob/mcf027

Gillner S, Korn S, Roloff A (2015) Leaf-Gas Exchange of Five Tree Species at Urban Street Sites. Arboric Urban Forestry 41:113–124. https://doi.org/10.48044/jauf.2015.012

Grilo F, McPhearson T, Aleixo C, Santos-Reis M, Branquinho C (2025) Urban trees through a functional traits' lens: Exploring the interplay between tree functional groups and social-ecological factors. Urban Forestry Urban Green 107:128749. https://doi.org/10.1016/j.ufug.2025.128749

IPCC (2021) Assessment Report 6 Climate Change 2021: The Physical Science Basis. In *IPCC*

IPCC (2023) Synthesis report of the ipcc sixth assessment report (AR6). Diriba Korecha Dadi. Panmao Zhai

Kendon M, McCarthy M, Jevrejeva S, Matthews A, Sparks T, Garforth J, Kennedy J (2022) State of the UK Climate 2021. Int J Climatol 42(S1):1–80. https://doi.org/10.1002/joc.7787

Kim K, Portis AR Jr. (2005) Temperature Dependence of Photosynthesis in Arabidopsis Plants with Modifications in Rubisco Activase and Membrane Fluidity. Plant Cell Physiol 46(3):522–530. https://doi.org/10.1093/pcp/pci052

Kullberg AT, Feeley KJ (2024) Seasonal acclimation of photosynthetic thermal tolerances in six woody tropical species along a thermal gradient. Funct Ecol 38(11):2493–2505. https://doi.org/10.1111/1365-2435.14657

Kunert N, Hajek P, Hietz P, Morris H, Rosner S, Tholen D (2022) Summer temperatures reach the thermal tolerance threshold of photosynthetic decline in temperate conifers. Plant Biol 24(7):1254–1261. https://doi.org/10.1111/plb.13349

Kuznetsova A, Brockhoff PB, Christensen RHB (2017) lmerTest Package: Tests in Linear Mixed Effects Models. J Stat Softw 82(13). https://doi.org/10.18637/jss.v082.i13

Lenth RV (2017) emmeans: Estimated Marginal Means, aka Least-Squares Means (p. 1.11.2-8) [Data set]. https://doi.org/10.32614/CRAN.package.emmeans

Leon-Garcia IV, Lasso E (2019) High heat tolerance in plants from the Andean highlands: Implications for paramos in a warmer world. PLoS ONE 14(11):e0224218. https://doi.org/10.1371/journal.pone.0224218

Mächler M, Rousseeuw P, Struyf A, Hubert M, Hornik K (2012) Cluster: Cluster Analysis Basics and Extensions. In *R packages* (Vol. 1)

Meier F, Scherer D (2012) Spatial and temporal variability of urban tree canopy temperature during summer 2010 in Berlin, Germany. Theoret Appl Climatol 110(3):373–384. https://doi.org/10.1007/s00704-012-0631-0

Münchinger IK, Hajek P, Akdogan B, Caicoya AT, Kunert N (2023) Leaf thermal tolerance and sensitivity of temperate tree species are correlated with leaf physiological and functional drought resistance traits. J Forestry Res 34(1):63–76. https://doi.org/10.1007/s11676-022-01594-y

Murchie EH, Lawson T (2013) Chlorophyll fluorescence analysis: A guide to good practice and understanding some new applications. J Exp Bot 64(13):3983–3998. https://doi.org/10.1093/jxb/ert208

Oksanen J, Simpson GL, Blanchet FG, Kindt R, Legendre P, Minchin PR, O'Hara RB, Solymos P, Stevens MHH, Szoecs E, Wagner H, Barbour M, Bedward M, Bolker B, Borcard D, Carvalho G, Chirico M, Caceres MD, Durand S, Borman T (2025) *vegan: Community Ecology Package* (Version 2.6–10) [Computer software]. https://cran.r-project.org/web/packages/vegan/index.html

Opti-Sciences (2013) OS5p+ User's Guide. www.optsci.com

O'sullivan OS, Heskel MA, Reich PB, Tjoelker MG, Weerasinghe LK, Penillard A, Zhu L, Egerton JJG, Bloomfield KJ, Creek D, Bahar NHA, Griffin KL, Hurry V, Meir P, Turnbull MH, Atkin OK (2017) Thermal limits of leaf metabolism across biomes. Glob Change Biol 23(1):209–223. https://doi.org/10.1111/gcb.13477

Perez TM, Feeley KJ (2020b) Photosynthetic heat tolerances and extreme leaf temperatures. Funct Ecol 34(11):2236–2245. https://doi.org/10.1111/1365-2435.13658

Posch BC, Hammer J, Atkin OK, Bramley H, Ruan Y-L, Trethowan R, Coast O (2022) Wheat photosystem II heat tolerance responds dynamically to short- and long-term warming. J Exp Bot 73(10):3268. https://doi.org/10.1093/jxb/erac039

R Core Team (2025) *R:* A Language and Environment for Statistical Computing [Computer software]. R Foundation for Statistical Computing. https://www.R-project.org/

Sharkey TD (2005) Effects of moderate heat stress on photosynthesis: Importance of thylakoid reactions, rubisco deactivation, reactive oxygen species, and thermotolerance provided by isoprene. Plant Cell Environ 28(3):269–277. https://doi.org/10.1111/j.1365-3040.2005.01324.x

Slot M, Cala D, Aranda J, Virgo A, Michaletz ST, Winter K (2021) Leaf heat tolerance of 147 tropical forest species varies with elevation and leaf functional traits, but not with phylogeny. Plant Cell Environ 44(7):2414–2427. https://doi.org/10.1111/pce.14060

Teskey R, Wertin T, Bauweraerts I, Ameye M, Mcguire MA, Steppe K (2015) Responses of tree species to heat waves and extreme heat

events. Plant Cell Environ 38(9):1699–1712. https://doi.org/10.1111/pce.12417

Tiwari R, Gloor E, da Cruz WJA, Schwantes Marimon B, Marimon-Junior BH, Reis SM, de Souza IA, Krause HG, Slot M, Winter K, Ashley D, Béu RG, Borges CS, Da Cunha M, Fauset S, Ferreira LDS, Gonçalves MDA, Lopes TT, Marques EQ, Galbraith D (2021) Photosynthetic quantum efficiency in south-eastern Amazonian trees may be already affected by climate change. Plant Cell Environ 44(7):2428–2439. https://doi.org/10.1111/pce.13770

Treezilla T (2024) *Treezilla*. https://treezilla.org/

Zecchin B, Caudullo G, de Rigo D (2016) Acer campestre in Europe: Distribution, habitat, usage and threats